The existence of the edge region of the Antarctic stratospheric vortex

Howard K. Roscoe,[1] Wuhu Feng,[2] Martyn P. Chipperfield,[2] Miriam Trainic,[3] and Emily F. Shuckburgh[1]

Received 10 March 2011; revised 14 December 2011; accepted 14 December 2011; published 16 February 2012.

[1] New evidence from models, ozone measurements and balloon trajectories is presented that confirms the existence of a broad cohesive region of air at the edge of the Antarctic stratospheric vortex that is only weakly mixed with the core of the vortex. Comprehensive measurements by Antarctic ozonesondes in 2003 show quite different evolution in the edge region than in the core. With one exception, long duration balloons launched from Antarctica in spring 2005 remained confined to either the edge region of the vortex or its core. Calculations of effective diffusivity for 2003 and 2005 show similarly weak mixing in the edge region as earlier calculations for 1996. They again show that the edge region is a significant proportion of the area of the ozone hole. Its importance lies in the possibility that, unmixed, it can have more polar stratospheric clouds during the course of the 21st century, thereby delaying the recovery of the ozone hole.

Citation: Roscoe, H. K., W. Feng, M. P. Chipperfield, M. Trainic, and E. F. Shuckburgh (2012), The existence of the edge region of the Antarctic stratospheric vortex, *J. Geophys. Res.*, *117*, D04301, doi:10.1029/2011JD015940.

1. Introduction

[2] A UV-visible spectrometer of the SAOZ design [*Pommereau and Goutail*, 1988] was installed in 1991 near the Antarctic circle, at the British Antarctic Survey's station at Faraday (65.3°S), since renamed Vernadsky. The use of visible light for ozone measurements meant that ozone could be observed at this latitude throughout winter. This location is frequently in the stratospheric vortex, where the ozone hole occurs each year. The measurements from Faraday led to the conclusion that ozone loss starts in midwinter [*Roscoe et al.*, 1997], rather than later in spring as had been supposed from previous measurements further south despite previous predictions of midwinter loss [*Tuck*, 1989; *Solomon et al.*, 1993].

[3] These observations also led to the realization that ozone-poor air from the sunlit edge of the vortex was not exported to the vortex core in winter, leading to the supposition that an edge region of the vortex must exist, as previously identified [e.g., *Toon et al.*, 1989], that was poorly mixed with the vortex core. This supposition was reinforced by calculations using the SLIMCAT chemistry-transport model [*Chipperfield et al.*, 1996], in which transport along isentropic surfaces was driven by horizontal winds obtained from UK Met Office (UKMO) analyses: (1) calculations of total ozone for the winter of 1994 agreed remarkably well with the Faraday observations from that year [*Roscoe et al.*, 1997]; (2) calculations for 1996 showed that ozone loss originating within 60 to 65°S Potential Vorticity (PV)-equivalent latitude was not transported southward of 70° [*Lee et al.*, 2001]; and (3) measurements of ozone at specific altitudes by Antarctic ozonesondes in 1996 agreed well with the calculations [*Lee et al.*, 2000], although gaps in the ozonesonde data were large enough to prevent complete validation.

[4] Maps of the calculated ozone loss also showed that the edge region was between 5 and 15° latitude wide, as suggested elsewhere [e.g., *Rosenlof et al.*, 1997]. This is broad enough to be about half the area of the current ozone hole for much of the spring.

[5] This view of weak mixing was backed by calculations of effective diffusivity. Effective diffusivity k_{eff} [*Nakamura*, 1996] quantifies the large-scale irreversible mixing of a tracer by considering the enhancement to diffusion that arises through the stretching and folding of tracer contours by the atmospheric flow. Key to the derivation of the effective diffusivity is a consideration of the evolution of tracer contours in a coordinate system based on equivalent latitude. The equivalent latitude, φ_e, of a tracer contour is the value of the latitude circle that encloses an equal area A_e [*Butchart and Remsberg*, 1986]. The diffusion enhancement factor is $(L_{eq}/L_{min})^2$, where L_{eq} is the so-called equivalent length of the stretched and folded tracer contour and L_{min} is the circumference of the equivalent latitude circle (which is the minimum length of a tracer contour containing the same area). The effective diffusivity is then given by:

$$k_{eff} = k\left(L_{eq}/L_{min}\right)^2$$

where k is the background small-scale diffusivity.

[1]British Antarctic Survey, Cambridge, UK.
[2]School of Earth and Environment, University of Leeds, Leeds, UK.
[3]Imperial College, London, UK.

0148-0227/12/2011JD015940

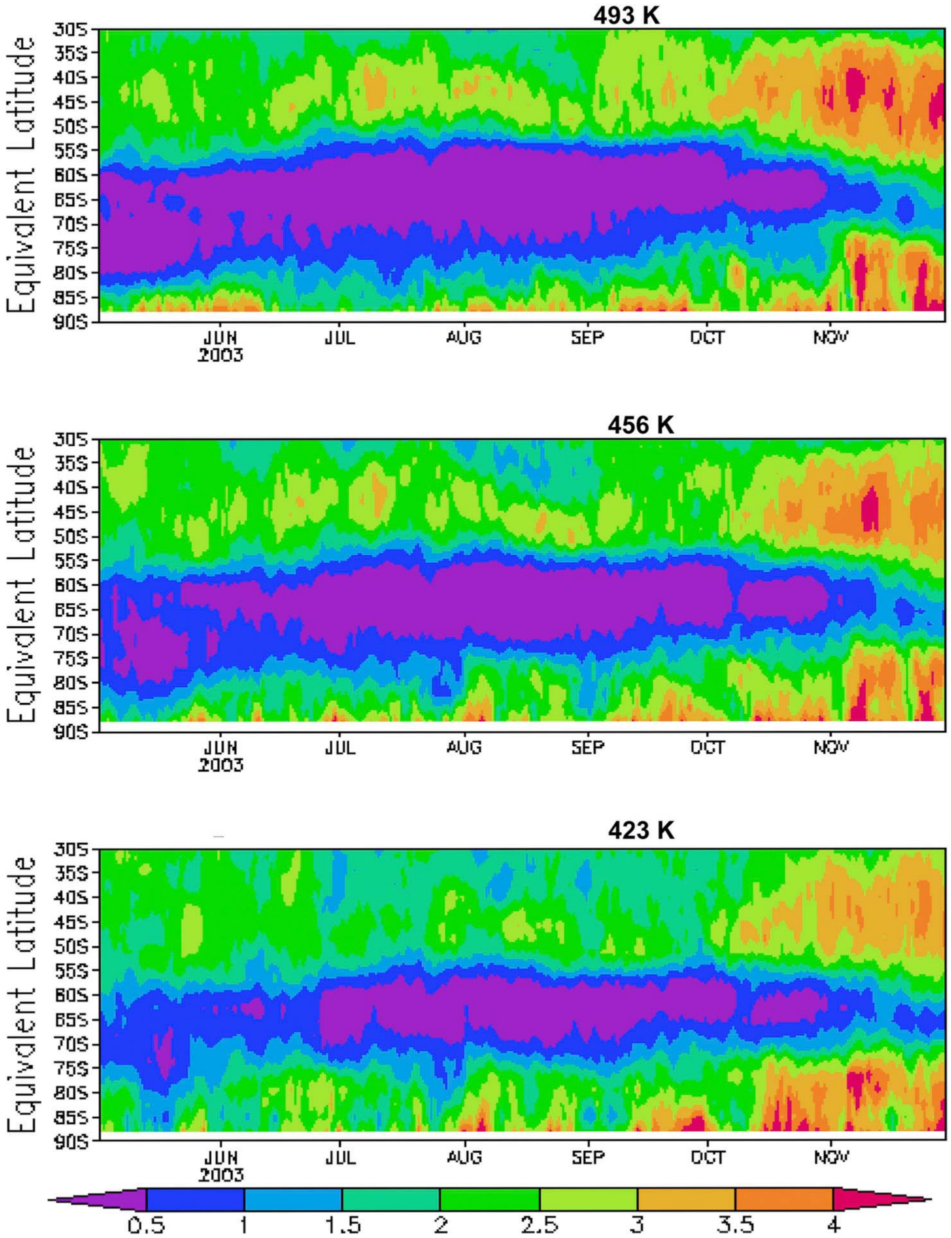

Figure 1. Contours of lognormalized equivalent length of effective diffusivity, calculated for the year 2003, plotted against the commonly used vortex-following coordinate PV-equivalent latitude, at the three potential temperatures of 493 K, 456 K, and 423 K (approximately 20, 17 and 13 km respectively). The tick marks for months define the 1st of the month in each label. The calculation uses equation (1), hence the units are logarithmic and zero is no mixing. Note that 2003 is the year of the QUOBI project discussed in section 3 and Figures 5, 6, and 7.

[6] In an equivalent-latitude coordinate system, the advection–diffusion equation for a passive tracer, q, is given by [*Nakamura*, 1996; *Shuckburgh and Haynes*, 2003]:

$$\partial q(\varphi_e,t)/\partial t = (\partial/\partial\varphi_e)\left(k\left(L_{eq}/L_{min}\right)^2\cos\varphi_e(\partial q/\partial\varphi_e)\right)/\left(R^2\cos\varphi_e\right)$$

where

$$L_{eq}^2(\varphi_e,t) = (\partial q/\partial A_e)^{-2}(\partial/\partial A_e)\int_{A\le Ae}|\text{Grad } q|^2\, dA$$

and

$$L_{min}^2(\varphi_e) = (2\pi R\cos\varphi_e)^2$$

Here R is the radius of the Earth. These equations provide a method for calculating the effective diffusivity as a function of equivalent latitude and time from an evolving tracer field by calculating the appropriate integrals and derivatives of the instantaneous tracer field (see *Haynes and Shuckburgh* [2000a] for more details). The units are often simplified

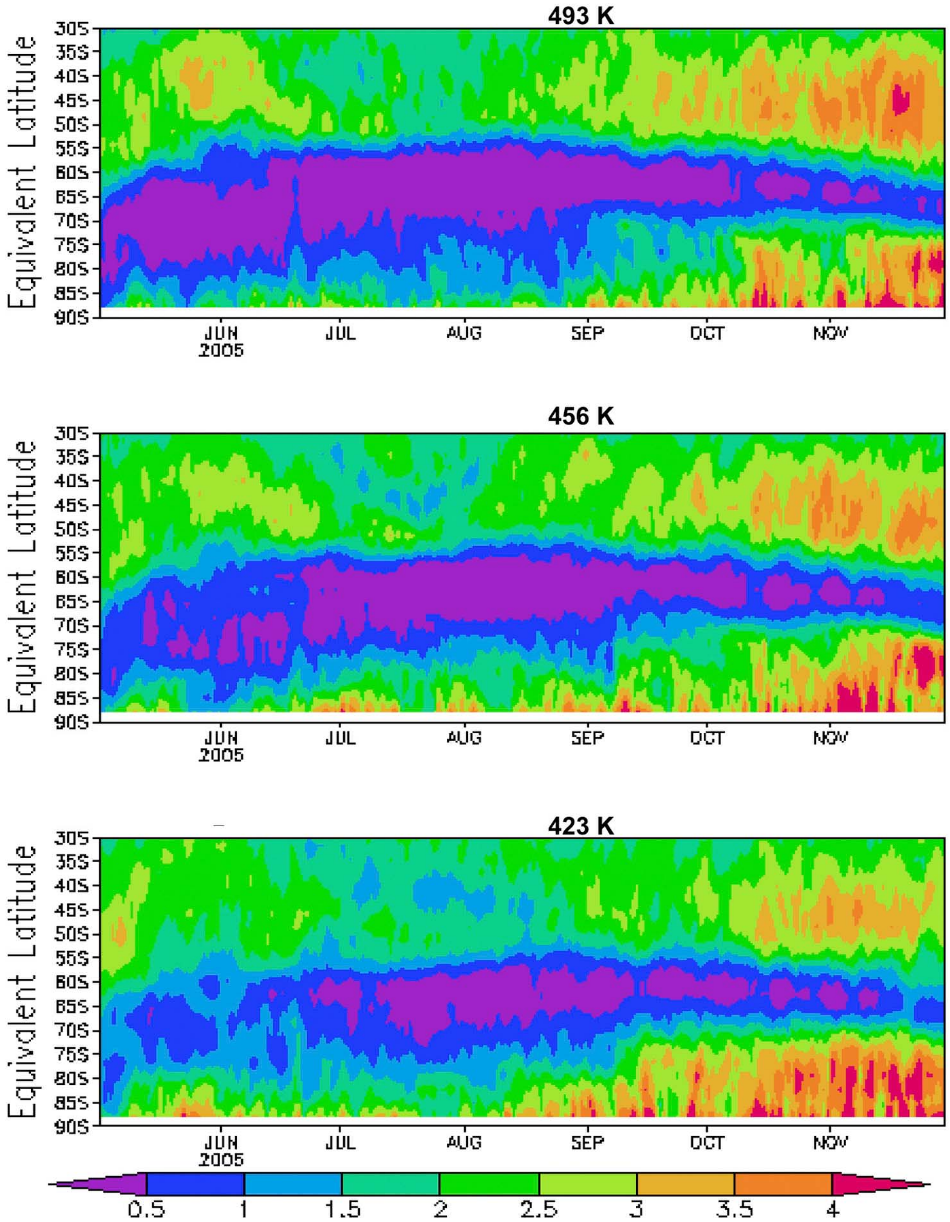

Figure 2. Same as Figure 1 but for 2005. This is the year of the VORCORE project discussed in section 4, and in Figures 8, 9, and 10.

[e.g., *Haynes and Shuckburgh*, 2000a] by calculating the lognormalized equivalent length of effective diffusivity:

$$\Lambda_{eq} = \ln\left(L_{eq}/L_{min}\right)^2 \quad (1)$$

so that a value of zero for the lognormalized equivalent length implies a tracer whose contour is still circular – i.e., zero mixing in the meridional direction. This also means that the relative magnitude of the effective diffusivity at different locations and times can be compared in circumstances where the small scale diffusivity k is unknown but assumed to be constant.

[7] In the above study by *Lee et al.* [2001], PV was used as the tracer as pioneered by *Haynes and Shuckburgh* [2000b], and its evolution on isentropic surfaces was calculated for 1996, again using UKMO horizontal winds. Maps of log-normalized equivalent length showed a broad region of $\Lambda_{eq} < 0.8$ between PV-equivalent latitudes of about 60°S and 70°S – about half the area within the vortex. The width of the edge region, defined by the Λ_{eq} contour of 0.8, remained constant until November, after which it showed signs of thinning, some weeks ahead of the vortex break-up in early December.

[8] Another analysis of ozone profiles measured near the edge of the Antarctic vortex seemed not to demonstrate such weak mixing with the vortex core, although it was Marambio [*Karhu et al.*, 2003] and the observations may not have been able to fully demonstrate mixing or its absence. However, this is a site that is more often completely outside

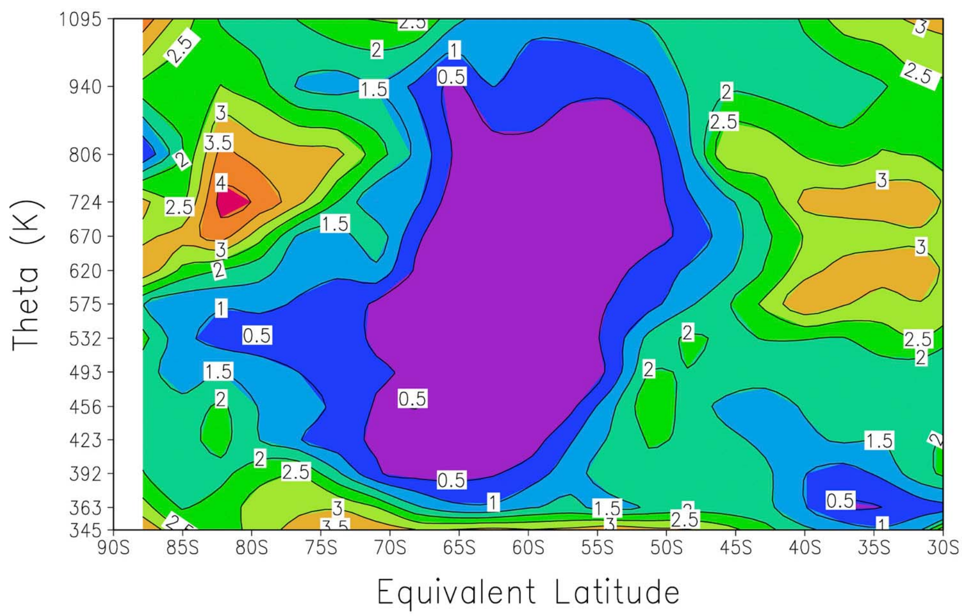

Figure 3. Contours of equivalent length of effective diffusivity on 23 July 2005, plotted against potential temperature θ (height) and the vortex-following coordinate PV-equivalent latitude. This is the year of the VORCORE project discussed in section 4, and in Figures 8, 9, and 10.

the vortex than Faraday, and the edge region was defined other than by effective diffusivity.

[9] The importance of the edge region's existence lies in the possibility that, unmixed, it can have more polar stratospheric clouds during the 21st century [*Roscoe and Lee*, 2001]. This can arise because it is warmer in the edge region than in the vortex core, and so it is not saturated in PSCs in winter and early spring, unlike the vortex core [*Cacciani et al.*, 1997]. Hence the cooling of the stratosphere as concentrations of greenhouse gases increase could give rise to more PSCs in the edge region, and so to more ozone loss despite the success of the Montreal Protocol, a result which would not be possible if the edge region and vortex core were strongly mixed, as then the large amounts of reactive chlorine currently produced in the vortex core would be mixed throughout the vortex, destroying ozone everywhere within the vortex boundary. Such a result would delay the recovery of the ozone hole.

[10] Here, we present new evidence for the existence of the edge region of the Antarctic vortex, as a broad edge region weakly mixed with the vortex core as found by *Lee et al.* [2001] – evidence from calculations of effective diffusivity in more years, from a comprehensive set of ozonesonde measurements and model calculations, and from the trajectories of pressurized long-duration balloons in the Antarctic vortex. We discuss the model calculations of effective diffusivity first because the results inform our analysis of the measurements.

2. Evidence From More Calculations of Effective Diffusivity

[11] We have made new calculations of effective diffusivity for the years 2003 and 2005, as part of the projects discussed in sections 3 and 4. The calculations were made using a tracer field from the SLIMCAT model. This version used a hybrid sigma-θ vertical coordinate from the surface to ~60 km [*Chipperfield*, 2006]. The horizontal winds and temperatures are specified using ECMWF operational meteorological analyses. Vertical advection in the θ-level domain is calculated from diabatic heating rates using a radiation scheme from NCAR [*Briegleb*, 1992], which gives a better representation of vertical transport [*Feng et al.*, 2005] and age-of-air [*Chipperfield*, 2006] than previous schemes. Chemical tracers in SLIMCAT are advected using the scheme of *Prather* [1986], which conserves second-order moments. The model was initialized from a SLIMCAT 5.6 x 5.6 degrees multiannual simulation [*Chipperfield*, 1999].

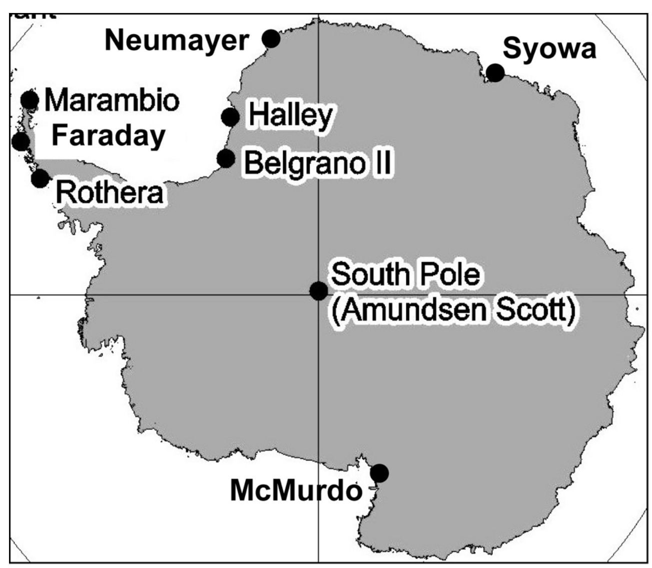

Figure 4. Map of Antarctica showing locations of some sites mentioned in the text.

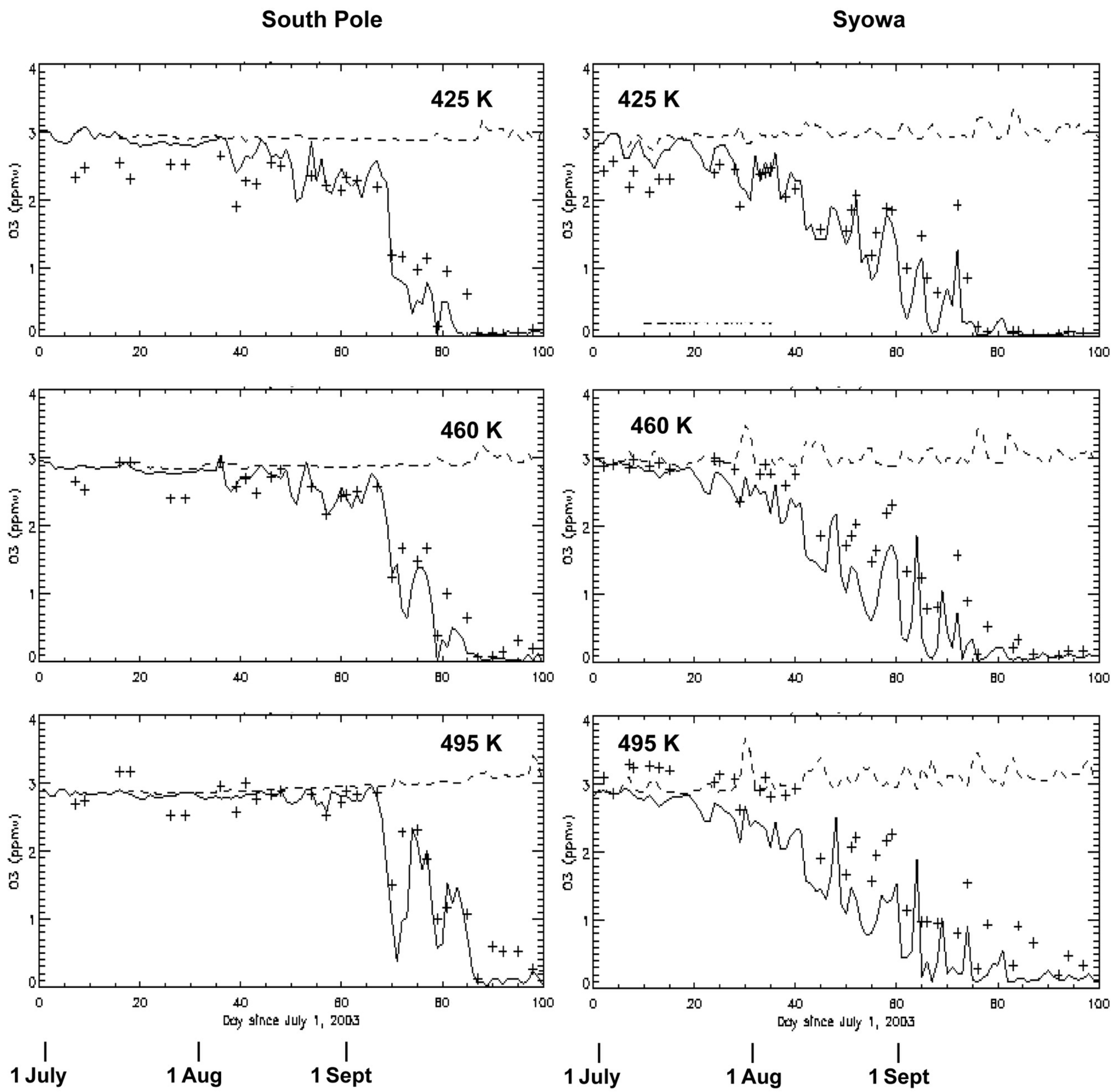

Figure 5. Measurements of ozone (ppmv) by sondes in 2003 (plus symbols) at (top) a potential temperature of 425 K, (middle) 460 K, and (bottom) 495 K, compared with calculations by the SLIMCAT model (solid lines), for (left) South Pole in the vortex core and (right) Syowa (69.0°S) in the edge region. Dashed lines show the model calculation of the ozone that would have existed in the absence of chemical loss. Very little ozone loss occurs at South Pole until after 1 September when the sun rises in the core of the vortex, whereas loss starts at the sunlit edge region at Syowa soon after midwinter. Hence no ozone-poor air is mixed from the edge region to the core for at least a month.

[12] The runs used here are at 2.8° latitude and 2.8° longitude horizontal resolution. The effective diffusivities are calculated using equation (1), from the simulated N_2O tracer. Our new calculations demonstrate that the weak mixing diagnosed for 1996 was not a one-off event for that year only. Figures 1 and 2 show the results. Again using the value of L_{eq} less than 0.8 to define the edge region, it has a width of almost 15° in equivalent latitude from mid-winter to mid-spring, then narrows progressively until its near-disappearance in November. In both years, the near-disappearance occurs well in advance of the vortex breakup later in December (not shown).

[13] The vortex edge by its conventional definition from PV gradients [*Nash et al.*, 1996] usually lies within the edge region as defined above by effective diffusivity. However, maps of chemical ozone loss show that the edge region lies wholly within the ozone hole, as originally shown in the model calculations from *Roscoe et al.* [1997].

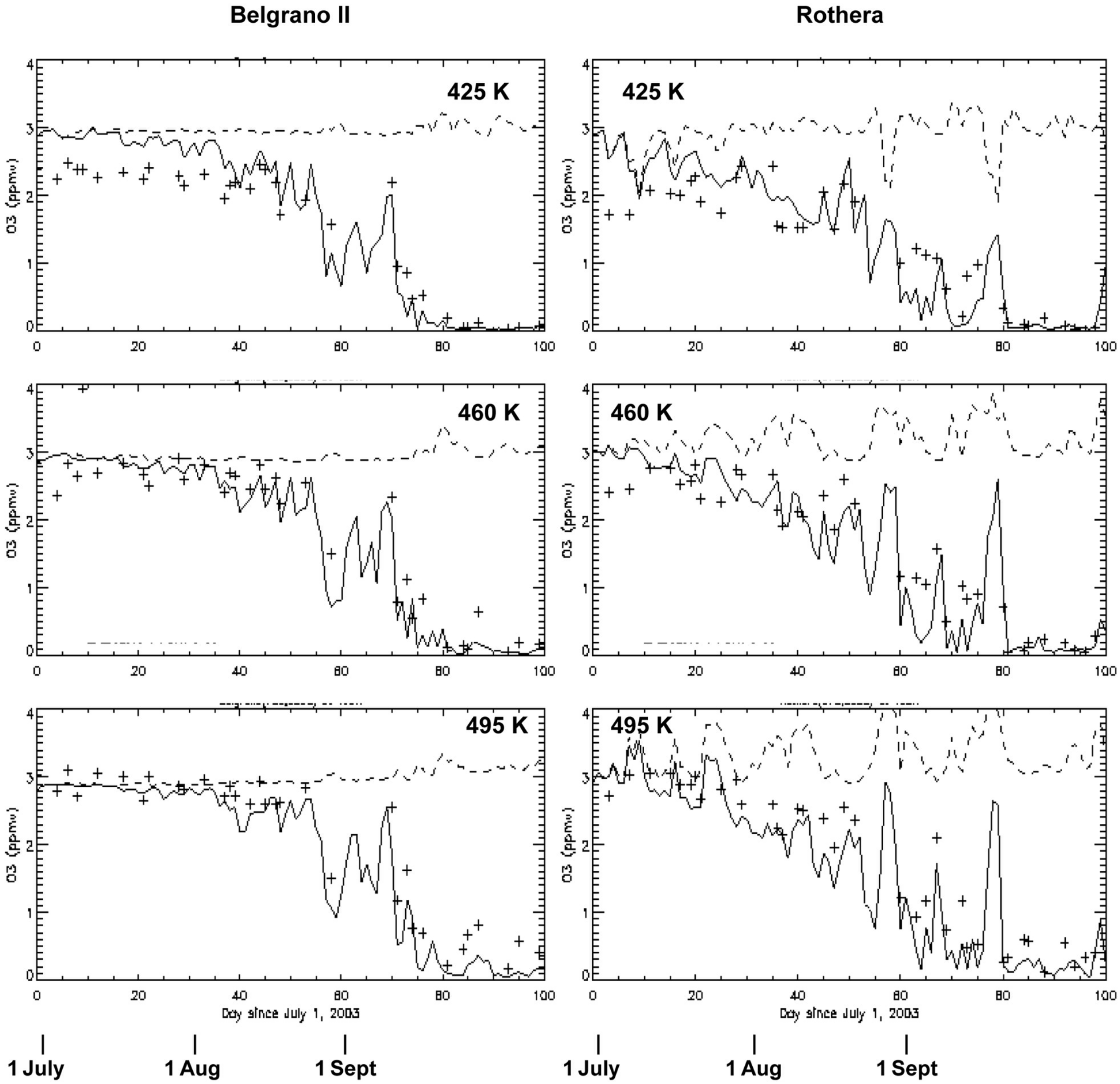

Figure 6a. Same as Figure 5 but for (left) Belgrano II (77.9°S) in the vortex core and (right) Rothera (67.6°S) in the edge region. Unlike Figure 5 (left), ozone loss at Belgrano II starts somewhat earlier than at South Pole – near the end of August when the sun rises at Belgrano II. Unlike Figure 5 (right), Rothera has frequent episodes when it is outside the vortex, characterized by larger amounts of passive ozone (dashed lines) at (top) 494 K and (middle) 460 K, and (bottom) smaller amounts of passive ozone at 425 K.

[14] The vertical profile of the edge region is shown in Figure 3. The contour of L_{eq} equal to 0.8 displays the well-known equatorward tilt of the vortex with increasing height. It is this tilt that demands vertical interpolation of the effective diffusivity when calculating equivalent lengths at specific altitudes in section 4.

3. New Evidence From Ozonesonde Measurements and Models

[15] In 2003, a large number of ozonesondes were flown in Antarctica as part of the EU-funded project Quantitative Understanding of Ozone losses by Bipolar Investigations (QUOBI) [*Parrondo et al.*, 2007; *Tripathi et al.*, 2007]. This project coordinated the sonde launches to provide two or more measurements of the same air mass separated in time, in order to infer chemical ozone loss occurring along a trajectory (the so-called Match technique), and to compare the ozone loss to model calculations [*Feng et al.*, 2005; *Tripathi et al.*, 2007].

[16] A by-product that resulted was a dense time series of ozone profiles at each Antarctic site, and model calculations for comparison. Here, we show the time series of ozone from South Pole, Belgrano II (77.9°S), Neumayer (70.6°S),

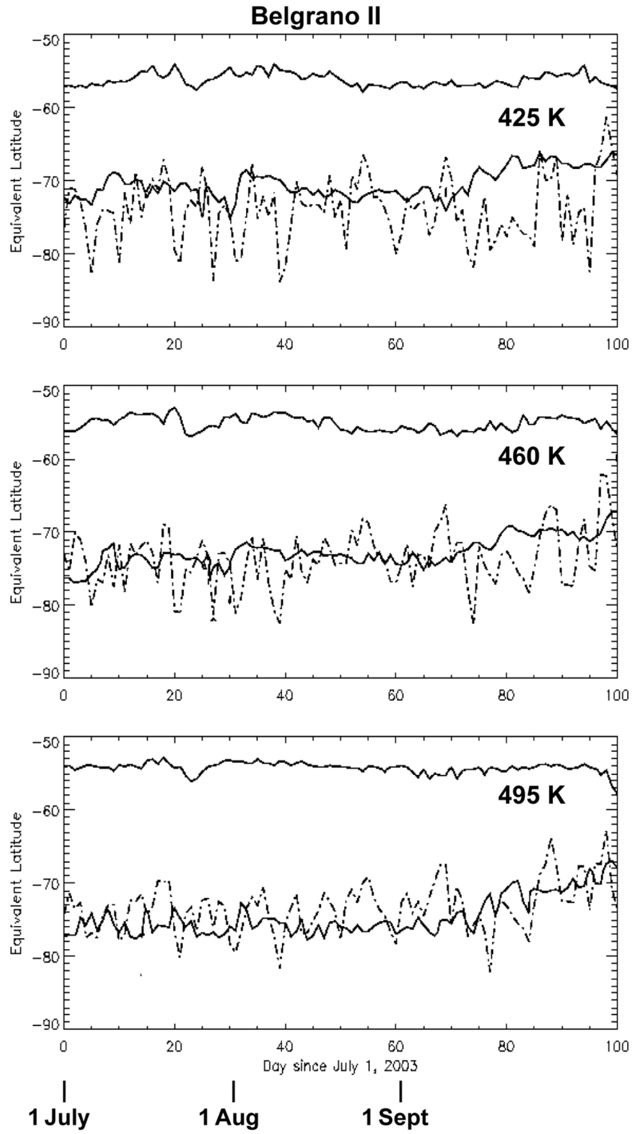

Figure 6b. The location of the station Belgrano II (77.9°S) in Equivalent Latitude coordinates (dash-dotted line), together with the Equivalent Latitudes of the extremes of the edge region of the vortex defined by lognormalized equivalent length of effective diffusivity = 0.8 (solid lines).

Syowa (69.0°S), Rothera (67.6°S) and Marambio (64.2°S) – see Figure 4 for a map of locations. These sites are selected because they span a range of periods within the vortex core, the edge region, and outside it: the results of effective diffusivity calculations described in section 2 showed us that some sites are almost always in the vortex core (e.g., South Pole), some alternate between the core and the edge region (e.g., Belgrano II, Neumayer), some are almost always in the edge region (e.g., Syowa), and some alternate between the edge region and outside the vortex (e.g., Rothera, Marambio). The QUOBI ozone measurements shown here have not previously been published in this format.

[17] We also show comparisons with ozone mixing ratios from the run of SLIMCAT model for 2003 discussed in section 2. The measurements and model results at selected altitudes are shown in Figures 5, 6, and 7, where the timings of ozone loss demonstrate very good agreement. Both measurements and model show the gradual ozone loss in the edge region (Figures 5 (right), 6a (right) and 7 (right)) starting near 1 August, significantly earlier that in the vortex core. They conclusively demonstrate that this edge region air is not mixed to the vortex core (Figure 5, left), as similarly concluded from methane and other measurements by *Russell et al.* [1993], and as suggested by measurements from Dumont D'Urville by *Godin et al.* [2001]. In Figure 5 (left), ozone loss can be seen by eye to start two months later. Previous to this date the measurements and models show negligible ozone loss at South Pole. Belgrano II in Figure 6a is more complex, and as shown in Figure 6b it spends a small proportion of its time in the vortex edge region, more at higher altitudes, consistent with the ozone results in Figure 6a.

[18] Rothera (Figure 6a, right) shows some periods outside the vortex, easily discernable by eye in the figure because of the change in passive ozone between inside and outside the vortex. The dips in passive ozone at days 57 and 78 at Rothera at 425 K, compared to the increases at 460 K and above, are presumably where extra-vortex air has been mixed over Rothera, with its different passive-ozone profile. There are no sondes from Rothera on those days, but the model tells us that ozone went to values with small ozone loss (small difference between passive and active ozone), hence Rothera was almost fully outside the vortex on those days. Belgrano does not display this behavior in its passive ozone because it was never outside the vortex. Marambio (Figure 7, right) is also frequently in edge region air, but with longer periods outside the vortex than Rothera near days 57 and 78. The model tells us that the ozone loss was negligible on those days, so that Marambio must have been fully outside the vortex. Plots from Neumayer (Figure 7, left) are more difficult to interpret, as it is sometimes in the edge region and sometimes in the vortex core, and passive ozone is unchanged between the edge region and the core; however the lack of any dips in passive ozone at 425 K suggest that, like Belgrano, Neumayer was never outside the vortex.

[19] Figures 5 and 6a show one minor feature of disagreement between calculations and measurements. The vortex core calculations (solid lines, left columns) at 425 and 460 K show slightly more mixing than the measurements (plus symbols, left columns) - the calculations show reductions by eye of 5 to 10% in ozone during July and early August, whereas there is negligible change in measured ozone until 10 September at South Pole (Figure 5) and until 10 August at Belgrano II (Figure 6a). We are uncertain of the cause, but the model has a fairly coarse resolution (2.8° latitude × 2.8° longitude), at which numerical diffusion could contribute to an overestimate in mixing in the model, particularly at such small values of mixing.

4. Evidence From Trajectories of Long-Duration Antarctic Balloons

[20] In 2005, over 30 long-duration pressurized balloons were launched from McMurdo (77.9°S, Figure 4) as part of the VORCORE project [*Hertzog et al.*, 2007], funded by CNRS and CNES (France), and NSF (USA). The project plan was to investigate the small-scale dynamics of the vortex core by following the balloons as they were moved

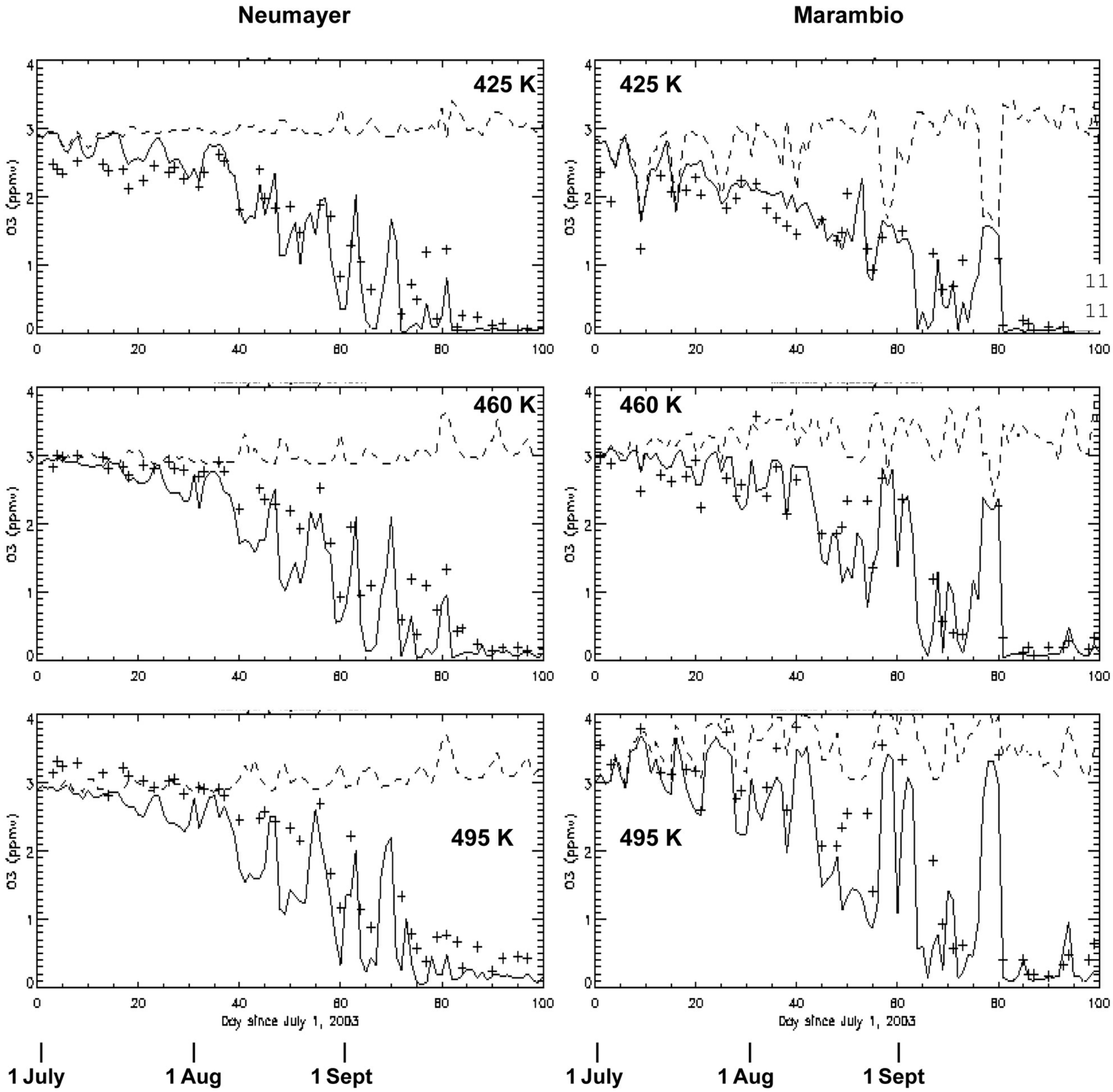

Figure 7. Same as Figure 5 but for (left) Neumayer (70.6°S), which alternates between the vortex core and the edge region, and (right) Marambio (64.2°S), which alternates between the edge region and being outside the vortex. The large excursions in ozone at Neumayer during August and early September show its alternation between the vortex core and the edge region. Marambio has more frequent and longer episodes when it is outside the vortex than Rothera in Figure 6a (right), and the periods outside the vortex are again characterized by larger amounts of passive ozone (dashed lines) at (top) 494 K and (middle) 460 K, and (bottom) smaller amounts of passive ozone at 425 K.

up and down by gravity waves, as well as the large-scale dynamics by following balloons until they reached midlatitudes. Hence the balloons carried GPS location sensors, as well as pressure transducers and other lightweight sensors. Positions were recorded every 15 min. Two sizes of balloon were available, aiming at 70 hPa or at 50 hPa. The nature of the pressurized skin of the balloon meant that flights were almost at constant density (isopycnal), although there were small vertical excursions with sunlight and darkness, particularly later in the spring. There were 23 flights that lasted more than 5 days.

[21] Following the VORCORE project plan, balloon launches were timed to attempt flights that started in the core of the stratospheric vortex. But despite its southerly location (Figure 4), McMurdo is often in the edge-region of the vortex, because of the frequent displacement of the vortex toward Halley and Rothera. This, coupled with the complex procedure for launching the balloons and delays by weather

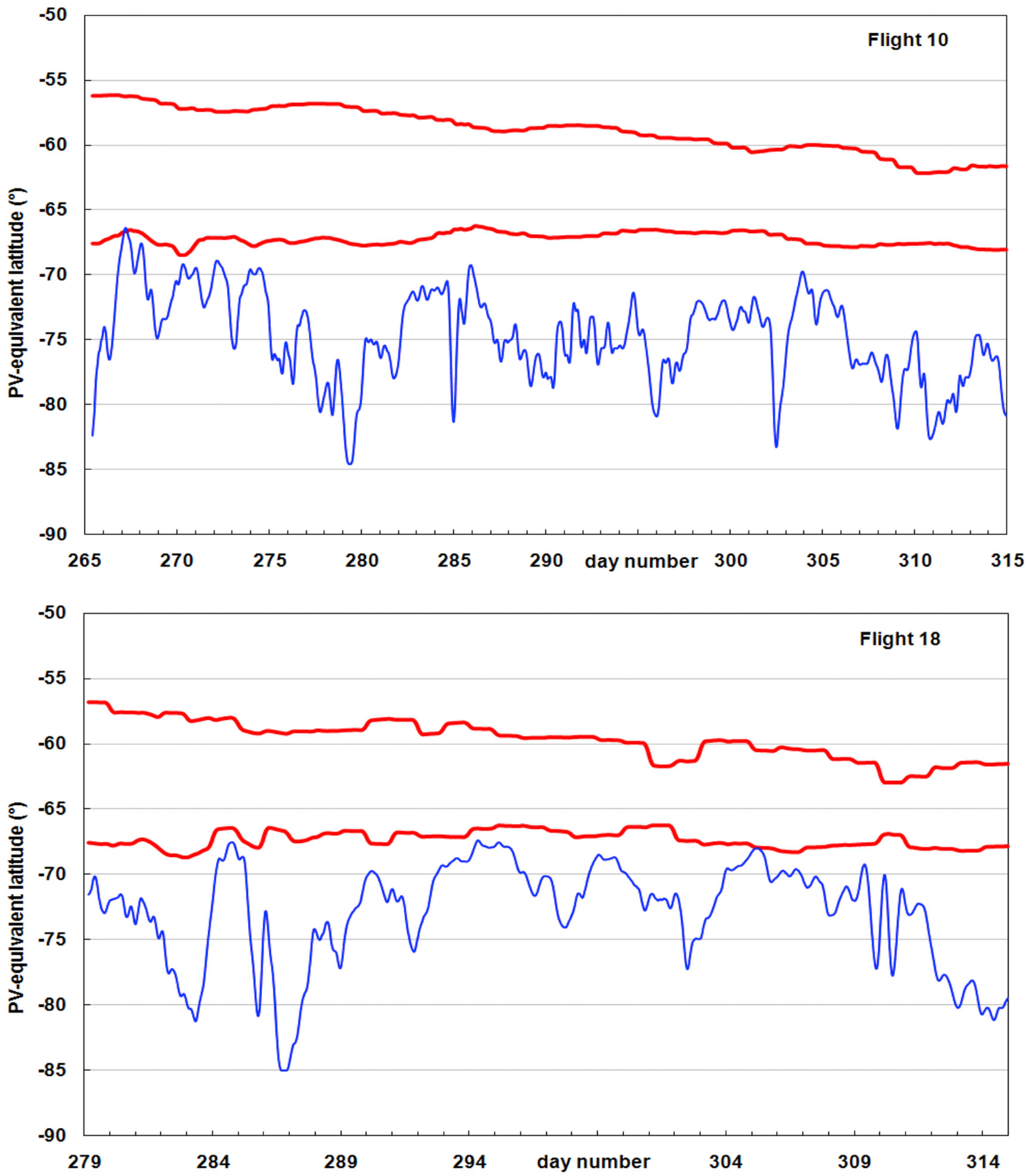

Figure 8. Locations of balloons of the VORCORE project in Antarctica in spring 2005, launched from McMurdo into the core of the stratospheric vortex on (top) 22 September (day 265), and (bottom) 5 October (day 278), each to 50 hPa. The red lines are the limits of the edge region of the vortex, as defined by an equivalent length of effective diffusivity of 0.8 (see section 2 and Figure 2 for effective diffusivity calculations and results). The blue lines are the balloon locations in the vortex-following coordinate of PV-equivalent latitude. All data is smoothed by a triangular function of full width half maximum 5 h.

on the ground, meant that some balloons were launched into edge-region air.

[22] In Figures 8, 9, and 10, we show balloon locations relative to the edge region, defined by an equivalent length of effective diffusivity of less than 0.8 (red lines). The original effective diffusivity calculations are those described in section 2, which follow tracer contours on isentropic surfaces as discussed in section 2. However, the balloons follow near-isopycnal surfaces, so are not at the potential temperatures of the model levels used in the calculations. Hence the limits of the edge region in Figures 8, 9, and 10 are vertically interpolated to the actual balloon height. The figures end at the date of the rapid increase in effective diffusivity evident in Figure 2 on 11 November 2005 (day 315).

[23] Most of the flights started in the vortex core and remained there, as in Figure 8. Also as in Figure 8, the balloons made considerable excursions in equivalent latitude – the mixing within the vortex core is far from zero, as predicted in Figures 1 and 2. This is by contrast to Figure 9, which shows the two flights that were launched into the edge

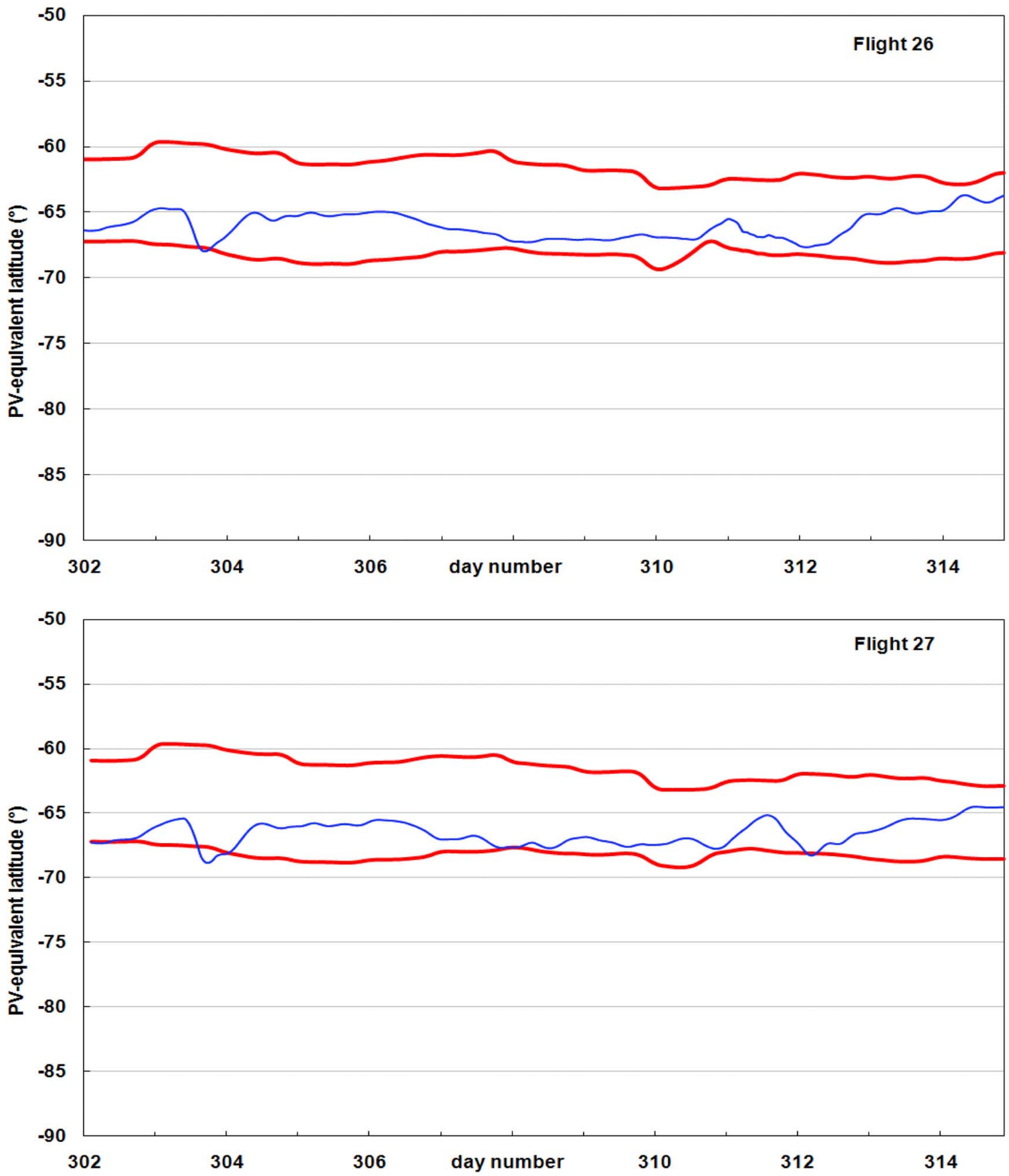

Figure 9. Same as Figure 8 but for balloons launched into the edge region of the stratospheric vortex on 28 October (day 301), hence the later start to the time axes than in Figure 7. Note that neither balloon moves irreversibly into the vortex core, and that their excursions in equivalent latitude are much less than the flights in Figure 6a.

region – here there is minimal excursion in equivalent latitude, showing weak mixing within the edge region itself as well as weak mixing to the vortex core. This is exactly the behavior predicted by the effective diffusivities shown in Figure 1.

[24] Some flights went a degree or so within our red lines defining the edge region for one or two days and then returned to the vortex core. This is very likely due to errors in the interpolation of effective diffusivity to balloon altitude, given the day-night vertical excursions and the tilt in the edge region shown in Figure 3. Only one flight of the 21 that started in the vortex core went irreversibly to the edge region (Figure 10). The fact of the balloon's smaller excursions in equivalent latitude in Figure 10, when apparently inside the edge region, is a compelling argument in favor of it having got there – its location in the edge region is not an illusion. We cannot appeal to the lower altitude of the balloon as the cause of this behavior, as other flights were also at 70 hPa but did not move from core to edge. We cannot exclude the possibility that a small vertical excursion in potential

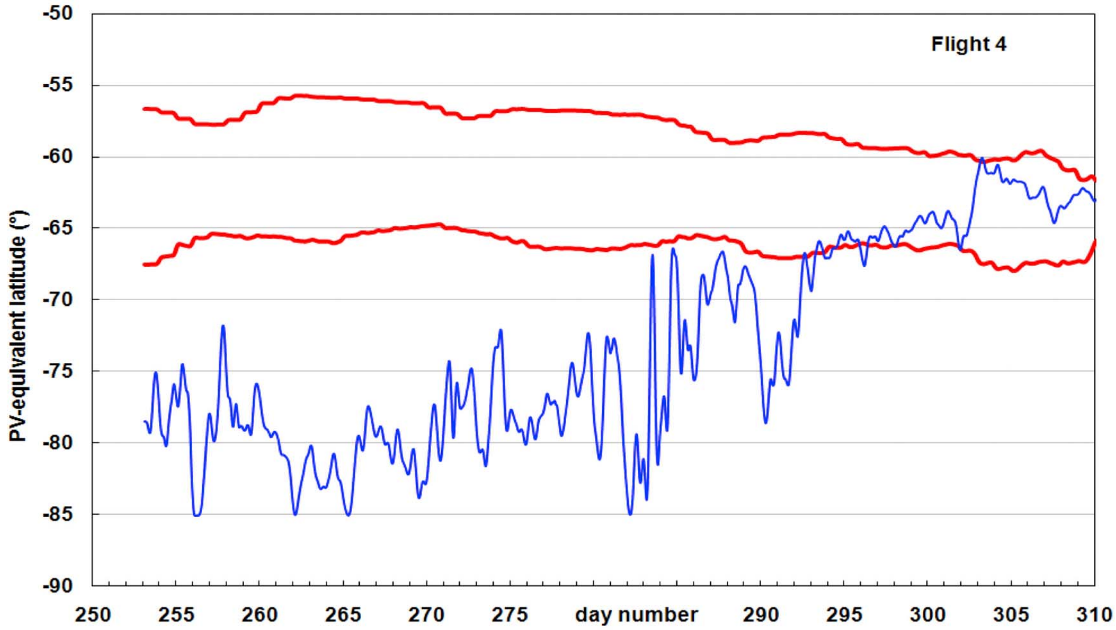

Figure 10. Same as Figure 8 but for the balloon launched into the vortex core on 9 September (day 252) to 70 hPa. This is the only flight of the 21 starting in the vortex core that went irreversibly to the edge region, demonstrating that although the mixing to the edge region is weak it is not zero. Note the smaller and less rapid excursions in equivalent latitude after the balloon enters the edge region on day 293 – the mixing within the edge region is significantly weaker than the mixing within the vortex core.

temperature, because of the isopycnal nature of the balloon, had moved it into edge-region air. However, we feel that it probably demonstrates that although the mixing is weak it is not zero.

5. Conclusions

[25] We have shown new measurements and calculations that greatly reinforce previous evidence for the existence of the edge region of the vortex in the Antarctic stratosphere. The measurements in 2003 and 2005 each show independently the existence of the edge region, as do the calculations for 2003 and 2005. Previous evidence was from measurements and calculations for 1994 and 1996, and measurements in 1987. The measurements and calculations are in a variety of styles and from a variety of sources, and are unequivocal that the edge region is only weakly mixed within itself and with the core of the vortex. However, we cannot assert that this conclusion is necessarily valid for all years – clearly it was not valid for at least part of the spring of 2002, when the vortex split into two parts [e.g., *Roscoe et al.*, 2005].

[26] The edge region is half the area of the ozone hole. The importance of its reconfirmed existence lies in the possibility that, if its temperature follows that of the global mean stratosphere, then unmixed it can have more polar stratospheric clouds during the 21st century [*Roscoe and Lee*, 2001], and so to more ozone loss despite the success of the Montreal Protocol. This could result in delays to the recovery of the ozone hole. Future work will investigate this possibility in detail.

[27] **Acknowledgments.** We thank the large number of participants in the QUOBI project who launched ozonesondes from Antarctic sites. QUOBI was funded by EC contract EVK2-2001-00129. We also thank the members of the VORCORE project from CNRS, LMD, CNES and NSF; we especially thank Albert Herzog and Francois Vial of LMD for their enthusiasm, and for the supply of VORCORE balloon data including their equivalent latitudes.

References

Briegleb, B. P. (1992), Delta-Eddington approximation for solar radiation in the NCAR community climate model, *J. Geophys. Res.*, *97*, 7603–7612.
Butchart, N., and E. E. Remsberg (1986), The area of the stratospheric polar vortex as a diagnostic for tracer transport on an isentropic surface, *J. Atmos. Sci.*, *43*, 1319–1339.
Cacciani, M., G. Fiocco, P. Colagrande, P. Di Girolamo, A. di Sarra, and D. Fua (1997), Lidar observations of polar stratospheric clouds at the South Pole: 1. Stratospheric unperturbed conditions, 1990, *J. Geophys. Res.*, *102*, 12,937–12,943, doi:10.1029/97JD00360.
Chipperfield, M. P. (1999), Multiannual simulations with a three-dimensional chemical transport model, *J. Geophys. Res.*, *104*, 1781–1805, doi:10.1029/98JD02597.
Chipperfield, M. P. (2006), New version of the TOMCAT/SLIMCAT off-Line chemical transport model: Intercomparison of stratospheric tracer experiments, *Q. J. R. Meteorol. Soc.*, *132*, 1179–1203, doi:10.1256/qj.05.51.
Chipperfield, M. P., M. L. Santee, L. Froidevaux, G. L. Manney, W. G. Read, J. W. Waters, A. E. Roche, and J. M. Russell (1996), Analysis of UARS data in the southern polar vortex in September 1992 using a chemical transport model, *J. Geophys. Res.*, *101*, 18,861–18,881, doi:10.1029/96JD00936.
Feng, W., et al. (2005), Three-dimensional model study of the Arctic ozone loss in 2002/03 and comparison with 1999/2000 and 2003/04, *Atmos. Chem. Phys.*, *5*, 139–152, doi:10.5194/acp-5-139-2005.
Godin, S., V. Bergeret, S. Bekki, C. David, and G. Megie (2001), Study of the interannual ozone loss and the permeability of the Antarctic polar vortex from aerosol and ozone lidar measurements in Dumont d'Urville (66.4°S, 140°E), *J. Geophys. Res.*, *106*, 1311–1330, doi:10.1029/2000JD900459.
Haynes, P. H., and E. F. Shuckburgh (2000a), Effective diffusivity as a diagnostic of atmospheric transport: 1. Stratosphere, *J. Geophys. Res.*, *105*, 22,777–22,794, doi:10.1029/2000JD900093.

Haynes, P. H., and E. F. Shuckburgh (2000b), Effective diffusivity as a diagnostic of atmospheric transport: 2. Troposphere and lower stratosphere, *J. Geophys. Res.*, *105*, 22,795–22,810, doi:10.1029/2000JD900092.

Hertzog, A., et al. (2007), Stratéole/Vorcore—Long-duration, superpressure balloons to study the Antarctic lower stratosphere during the 2005 winter, *J. Atmos. Oceanic Technol.*, *24*, 2048–2061, doi:10.1175/2007JTECHA948.1.

Karhu, J. A., P. Taalas, J. Damski, and J. Kaurola (2003), Vertical distribution of ozone at Marambio, Antarctic Peninsula, during 1987–1999, *J. Geophys. Res.*, *108*(D17), 4545, doi:10.1029/2003JD001435.

Lee, A. M., H. K. Roscoe, and S. Oltmans (2000), Model and measurements show Antarctic ozone loss follows edge of polar night, *Geophys. Res. Lett.*, *27*, 3845–3848, doi:10.1029/2000GL011441.

Lee, A. M., H. K. Roscoe, A. E. Jones, P. H. Haynes, E. F. Shuckburgh, M. J. Morrey, and H. C. Pumphrey (2001), The impact of the mixing properties within the Antarctic stratospheric vortex on ozone loss in spring, *J. Geophys. Res.*, *106*, 3203–3211, doi:10.1029/2000JD900398.

Nakamura, N. (1996), Two dimensional mixing, edge formation, and permeability diagnosed in an area coordinate, *J. Atmos. Sci.*, *53*, 1524–1537, doi:10.1175/1520-0469(1996)053<1524:TDMEFA>2.0.CO;2.

Nash, E. R., P. A. Newman, J. E. Rosenfield, and M. R. Schoeberl (1996), An objective determination of the polar vortex using Ertel's potential vorticity, *J. Geophys. Res.*, *101*, 9471–9478, doi:10.1029/96JD00066.

Parrondo, M. C., M. Yela, M. Gil, P. von der Gathen, and H. Ochoa (2007), Mid-winter lower stratosphere temperatures in the Antarctic vortex: Comparison between observations and ECMWF and NCEP operational models, *Atmos. Chem. Phys.*, *7*, 435–441, doi:10.5194/acp-7-435-2007.

Pommereau, J.-P., and F. Goutail (1988), Stratospheric O_3 and NO_2 observations in the summer polar circle in summer and fall 1988, *Geophys. Res. Lett.*, *15*, 895–897, doi:10.1029/GL015i008p00895.

Prather, M. J. (1986), Numerical advection by conservation of second-order moments, *J. Geophys. Res.*, *91*, 6671–6681, doi:10.1029/JD091iD06p06671.

Roscoe, H. K., and A. M. Lee (2001), Increased stratospheric greenhouse gases could delay recovery of the ozone hole and of ozone loss at Southern mid-latitudes, *Adv. Space Res.*, *28*, 965–970, doi:10.1016/S0273-1177(01)80025-9.

Roscoe, H. K., A. E. Jones, and A. M. Lee (1997), Midwinter start to Antarctic ozone depletion: Evidence from observations and models, *Science*, *278*, 93–96, doi:10.1126/science.278.5335.93.

Roscoe, H. K., J. D. Shanklin, and S. R. Colwell (2005), Has the Antarctic vortex ever split before 2002?, *J. Atmos. Sci.*, *62*, 581–588, doi:10.1175/JAS-3331.1.

Rosenlof, K. H., A. F. Tuck, K. K. Kelly, J. M. Russell III, and M. P. McCormick (1997), Hemispheric asymmetries in water vapor and inferences about transport in the lower stratosphere, *J. Geophys. Res.*, *102*, 13,213–13,234, doi:10.1029/97JD00873.

Russell, J. M., III, A. F. Tuck, L. L. Gordley, J. H. Park, S. R. Drayson, J. E. Harries, R. J. Cicerone, and P. J. Crutzen (1993), HALOE Antarctic observations in the spring of 1991, *Geophys. Res. Lett.*, *20*, 719–722, doi:10.1029/93GL00497.

Shuckburgh, E. F., and P. H. Haynes (2003), Diagnosing transport and mixing using a tracer-based coordinate system, *Phys. Fluids*, *15*, 3342, doi:10.1063/1.1610471.

Solomon, S., J. P. Smith, R. W. Sanders, L. Perliski, H. L. Miller, G. H. Mount, J. G. Keys, and A. L. Schmeltekopf (1993), Visible and near-ultraviolet spectroscopy at McMurdo Station, Antarctica: 8. Observations of nighttime NO_2 and NO_3 from April to October 1991, *J. Geophys. Res.*, *98*, 993–1000, doi:10.1029/92JD02390.

Toon, G. C., C. B. Farmer, L. L. Lowes, and P. W. Schaper, J.-F. Blavier, and R. H. Norton (1989), Infrared aircraft measurements of stratospheric composition over Antarctica during September 1987, *J. Geophys. Res.*, *94*, 16,571–16,596, doi:10.1029/JD094iD14p16571.

Tripathi, O. P., et al. (2007), Comparison of polar ozone loss rates simulated by one-dimensional and three-dimensional models with Match observations in recent Antarctic and Arctic winters, *J. Geophys. Res.*, *112*, D12307, doi:10.1029/2006JD008370.

Tuck, A. F. (1989), Synoptic and chemical evolution of the Antarctic vortex in late winter and early spring, 1987, *J. Geophys. Res.*, *94*, 11,687–11,737, doi:10.1029/JD094iD09p11687.

M. P. Chipperfield and W. Feng, School of Earth and Environment, University of Leeds, Leeds LS2 9JT, UK.

H. R. Roscoe and E. F. Schuckburgh, British Antarctic Survey, Madingley Road, Cambridge CB3 0ET, UK. (h.roscoe@bas.ac.uk)

M. Trainic, Imperial College, London SW1 2AZ, UK.